AGE (2014) 36:9728
DOI 10.1007/s11357-014-9728-y

A comprehensive study of myocardial redox homeostasis in naturally and mimetically aged rats

Tamer Cebe · Karolin Yanar · Pınar Atukeren · Tuna Ozan · Aylin Irmak Kuruç · Ahmad Kunbaz · Mustafa Erinç Sitar · Murat Mengi · Mehmet Şerif Aydın · Mukaddes Eşrefoğlu · Seval Aydın · Ufuk Çakatay

Received: 22 August 2014 / Accepted: 29 October 2014 / Published online: 11 November 2014

Abstract Age-related myocardial dysfunction has important implications with impaired redox homeostasis. Current study focused on investigation of redox homeostasis and histopathological changes in the myocardium of mimetically (MA), naturally aged (NA), and young control (YC) rats. Chronic D-galactose administration to young male Wistar rats (5 months old) was used to set up experimental aging models. We investigated 16 different oxidative damage biomarkers which have evaluated redox homeostasis of cellular macromolecules such as protein, lipid, and DNA. As a protein oxidation biomarker, advanced oxidation end products, protein carbonyl groups, protein-bound advanced glycation end products, dityrosine, kynurenine, and *N*-formylkynurenine concentrations in MA and NA rats were found to be significantly higher compared to those in YC rats. On the other hand, the levels of protein thiol groups were not significantly different between groups, whereas lipid peroxidation biomarkers such as conjugated diens, lipid hydroperoxides, and malondialdehyde in MA and NA rats were found to be significantly higher in comparison to those in YCs. For the assessment of oxidative DNA damage, we analyzed eight hydroxy-5′-deoxyguanosine concentrations of MA and NA groups which were higher than YCs. As an antioxidant status in the MA and NA groups, Cu–Zn superoxide dismutase, ferric reducing antioxidant power, and total thiol levels were lower than those in the YCs. Only nonprotein thiol levels were not significantly different. We also observed similar histopathological changes in MA and NA rats. We concluded that the mimetic aging model could be considered as a reliable experimental model for myocardial senescence.

Keywords Myocardial aging · D-Galactose · Protein oxidation · Lipid peroxidation · Antioxidant capacity · DNA oxidation

T. Cebe · T. Ozan · A. I. Kuruç · A. Kunbaz
Basic Sciences, Cerrahpaşa Faculty of Medicine, Istanbul University,
Istanbul, Turkey

K. Yanar · P. Atukeren · M. E. Sitar · S. Aydın · U. Çakatay (✉)
Department of Medical Biochemistry, Cerrahpaşa Faculty of Medicine, Istanbul University,
34098 Fatih, Istanbul, Turkey
e-mail: cakatay@yahoo.com

M. Mengi
Department of Physiology, Cerrahpaşa Faculty of Medicine, Istanbul University,
Istanbul, Turkey

M. Ş. Aydın · M. Eşrefoğlu
Department of Histology and Embryology, Bezmialem Vakif University Medical Faculty,
Istanbul, Turkey

Introduction

The process of aging in human body is both visible from outside skin and invisible inside as systemic organs develop dysfunction during lifetime. Aging is a well-recognized risk factor in the development of cardiovascular diseases, which are the primary cause of death and

disability in the elderly population (Sung and Dyck 2012). Increased arterial stiffness, elevated systolic pressure, lower heart rate and cardiac output, left ventricular hypertrophy, reduction in the synthesis as well as bioavailability of NO, increased calcification of aortic and mitral valves, and finally massive myocyte loss altogether converge toward deterioration of heart function (Venkataraman et al. 2013).

Accumulating experimental evidence has been clearly shown that chronic D-galactose exposure induces premature aging similar to natural aging in rodents (Aydın et al. 2012; Cebe et al. 2014; Kumar and Rizvi 2014; Sudheesh et al. 2010; Yanar et al. 2011). The underlying mechanism(s) responsible for D-galactose accelerating aging has been explained to be due to the result of the mitochondrial dysfunction caused by complex I deficiency, formation of high concentration of advanced glycation end products (AGE), and also the increase in the osmotic stress resulting from the reduction of galactose to galactitol (Yanar et al. 2011).

Although many theories have been proposed to explain the aging process, neither of them appears to be fully satisfactory (Sitar et al. 2013). It is commonly accepted that the impaired redox homeostasis due to increased formation of reactive oxygen species (ROS) is the major hallmark of the multifactorial process of aging (Jin 2010; Sitar et al. 2013; Uzun et al. 2013). The age-related myocardial dysfunction has important implications with regard to impaired redox homeostasis (Duicu et al. 2013; Judge et al. 2005). Superoxide radical ions and other ROS are known to be produced as inevitable by-products of normal aerobic metabolism in cardiac tissue, while ROS may have important roles in cellular functions, such as cell signaling; furthermore, it is clear that high levels of ROS cause impaired redox homeostasis (Fanin et al. 2013). There is growing evidence that increased mitochondrial ROS formation is particularly harmful for aging cells (Shinmura 2013). ROS can attack and damage cellular macromolecules such as DNA, RNA, and proteins (Shinmura 2013). Mitochondria have also been implicated in several human disorders including cardiac dysfunction, and they play an important role in both natural and mimetic aging processes. Recently, an age-related decline in complex I and V activity that correlated with increased oxidative damage has been reported in the aged mouse heart, although there was no change in the protein expression levels of these aged mice (Choksi and Papaconstantinou 2008).

Current study focused on variations between myocardial levels of protein, lipid, and DNA oxidation biomarkers, antioxidant status parameters, and histopathological changes in mimetically (MA), naturally aged (NA) rats, and also their respective young controls (YCs).

Material and methods

Chemicals and apparatuses

Unless otherwise specified, the chemicals were from the highest analytical grades that are available. All chemicals and reagents were purchased from Merck (Darmstadt, Germany) and Sigma-Aldrich (St Louis, MO, USA). Deionized water was used in the analytical procedures. All reagents were stored at +4 °C. The reagents were brought to room temperature for 20 min before being used. Centrifugation procedures for the analysis of various oxidative stress biomarkers were performed at +4 °C with the Sigma 3-18 KS centrifuge (SIGMA Laborzentrifugen GmbH, Osterode am Harz, Germany).

The oxidative damage biomarker profiles of myocardial tissue samples were manually analyzed by spectrophotometric and spectrofluorimetric methods with BioTek Synergy™ H1 Hybrid Multi-Mode Microplate Reader (BioTek US, Winooski, VT, USA). Early stage of lipid peroxidation in myocardial tissue samples was assessed using a second derivative spectroscopy technique on the same device.

Animal model and treatment protocol

The study was initially performed with 24 male Sprague–Dawley rats. All of the experimental studies were conducted according to the national laws of the Republic of Turkey. The ethical protocol of the current research was approved by the Ethics Committee of Istanbul University, Istanbul, Turkey (Ethics Committee Issue number 2011/162). Rats were housed in a temperature-controlled room (25±5 °C) with 12-h light–dark cycles. All of them were fed standard laboratory diet nutrient pellets containing fat, protein, and carbohydrates, and they had a free access to tap water. After 1 week of adaptation period, the experimental animals were divided into three groups. Both group I, young control (YC) rats (n=8; 5 months old), and group

II, naturally aged (NA) rats (n=8; 24 months old), were given daily intraperitoneal injections of NaCl (0.9 %) for 6 weeks, whereas group III, mimetically aged (MA) rats (n=8; chronologically 5 months old), was given daily intraperitoneal injections of D-galactose (60 mg/kg body weight) for 6 weeks. All animals were sacrificed 24 h later following the last D-galactose injection.

Preparation of tissue samples

When the experimental period was over, rats were sacrificed under anesthesia with ketamine (44 mg/kg)–xylazine (33 mg/kg) combination. The major heart vessels, valves, and atria were trimmed away, and the ventricles were cut open and rinsed free of blood. Left ventricles extracted from the rats were quickly washed in a cool 0.9 % NaCl solution and put on an ice-cold plate. Left ventricle samples were then immediately frozen in liquid N_2 until homogenization occurred. The homogenization procedure was performed mechanically in 10 % (*w/v*) homogenizing buffer (100 mM $KH_2PO_4{\cdot}K_2HPO_4$, pH 7.4, plus 0.1 % (*w/v*) digitonin).

A portion of the myocardial tissue was fixed for histological examination in 4 % paraformaldehyde in phosphate-buffered saline (PBS) for 3–4 h at 4 °C. The tissue samples were post-fixed in the same fixative overnight in order to prepare paraffin sections (30 % sucrose in 0.1 M PBS for 2 days after post-fixation). Serial coronal paraffin sections (5 μm thick) were being cut for H&E staining.

Preparation of test samples

Supernatant fractions were obtained by the centrifugation of the homogenates in 5000*g* for 10 min. During aliquot preparation, supernatant fractions were maintained at +4 °C in dim light. The supernatant fractions were divided into aliquots (one for each assay) and immediately stored at −80 °C (for 2 weeks maximum) for oxidative stress parameters. The investigated oxidative stress-related biomarkers are provided in Table 1.

Table 1 Oxidative stress-related parameters investigated

Type	Parameter
Protein oxidation biomarkers	Advanced oxidation protein products (AOPP)
	Protein carbonyl groups (PCO)
	Protein-bound advanced glycation end products (prAGEs)
	Protein thiol groups (P-SH)
	Protein-bound dityrosine (prDT)
	Protein-bound kynurenine (pr KYN)
	Protein-bound *N*-formylkynurenine (prN-FKYN)
Lipid peroxidation biomarkers	Lipid hydroperoxides (L-OOHs)
	Malondialdehyde (MDA)
	Conjugated diens (CDs)
Oxidative DNA damage biomarker	8-Hydroxy-2′-deoxyguanosine (8-OHdG)
Antioxidant capacity biomarkers	Cu–Zn superoxide dismutase (Cu–Zn SOD)
	Ferric reducing antioxidant power (FRAP)
	Total thiol groups (T-SH)
	Nonprotein thiol groups (NP-SH)

Analytical methods

Assays of protein oxidation markers

Advanced oxidation protein products Spectrophotometric analysis of advanced oxidation protein product (AOPP) concentrations was performed with slight modification of Hanasand's method (Hanasand et al. 2012). Samples were prepared in the following way: 10 μL of supernatant, 40 μL of PBS, and 200-μL citric acid solution (20 mmol/L) were mixed in a microplate. One minute later, 10 μL of 1.16 M potassium iodide was added to each microplate wells, and then, the absorbance of the reaction mixture was recorded at 340 nm against a reagent blank. The absorbance of chloramine-T standards was run in duplicate in order to increase the precision of the assay. The related absorbance was linear within the range of 0 to 100 μmol/L. AOPP concentration was expressed as micromoles per liter of chloramine-T equivalents. All readings were performed within 2 min after potassium iodide addition, for avoiding uncontrollable color development leads to possible deviation from the chloramine standard curve. The coefficients of intra- and inter-assay variations were 1.5 % (n=8) and 2.2 % (n=8), respectively. The AOPP-bovine serum albumin (BSA) positive control and untreated BSA were both prepared in vitro and tested according to the AOPP assay protocol (Zeng et al. 2014).

Protein carbonyl groups Protein carbonyl (PCO) assay was performed as described by Reznick and Packer

(1994), with some slight modifications in order to apply small volumes of myocardial tissue homogenates. PCO groups react with 2,4-dinitrophenylhydrazine (DNPH) reagent (100 μL supernatant/400 μL DNPH) to form chromophoric dinitrophenylhydrazones. DNPH was dissolved in HCl, and after DNPH reaction, proteins were precipitated with an equal amount of 20 % (*w/v*) trichloroacetic acid and washed three times with 400 μL of an ethanol/ethyl acetate mixture (1:1). Washing procedures were performed by mechanical disruption of pellets, and repelleting process was accomplished by centrifugation at 3000*g* for 5 min. Finally, the protein precipitates were dissolved in a 200-μL 6 M guanidine–HCl solution, and the results of the absorbance values were recorded at 360 nm using the molar extinction coefficient of DNPH, ε=22,000 M^{-1} cm^{-1}. The coefficients of intra- and inter-assay variations for modified carbonyl assay were 4.0 % (n=8) and 7.9 % (n=8), respectively. The PCO-BSA positive control and untreated BSA were both prepared according to the method of Lenarczyk et al. (2009) and tested according to the PCO assay protocol.

Protein-bound advanced glycation end products Determination of protein-bound advanced glycation end products (prAGEs) (i.e., some fluorescent products from the family of AGEs) was based on the spectrofluorimetric detection (Munch et al. 1997). We preferred to assay prAGEs for avoiding the possible interferences that may be derived from nonprotein constituents of the supernatant fraction. Tissue proteins of experimental animals were precipitated with trichloroacetic acid 100 g/L for 20 min on ice. After centrifugation for 15 min at 5000*g* and three washing steps with trichloroacetic acid 100 g/L, the pellets were redissolved and diluted (1:20) in PBS buffer, pH 7.4, and then used for fluorescence spectroscopy. Fluorescence intensity was expressed in fluorescence units (FU), and the results were given as FU per milligram protein. Supernatant fractions of tissue homogenates were diluted (1:20) with PBS, pH 7.4, and fluorescence intensity was recorded at the emission maximum (440 nm) upon excitation at 350 nm. The coefficients of intra- and inter-assay variations for modified prAGEs assay were 5.8 % (n=8) and 8.3 % (n=8), respectively. The AGE-BSA positive control and untreated BSA were both prepared according to the method of Wróbel et al. (1997) and tested according to the assay protocol.

Protein thiol groups The protein thiol (P-SH) groups were calculated by subtracting the nonprotein thiol (NP-SH) groups from total thiol (T-SH) groups.

Content of dityrosine, kynurenine, and N'-formylkynurenine We preferred to assay protein-bound dityrosine (prDT), protein-bound kynurenine (prKYN), and protein-bound *N*-formylkynurenine (prN-FKYN) for avoiding the possible interferences that may be derived from nonprotein constituents of tissue homogenates. Tissue proteins of experimental animals were precipitated with trichloroacetic acid 100 g/L for 20 min on ice. After centrifugation for 15 min at 5000*g* and three washing steps with trichloroacetic acid 100 g/L, the pellets were redissolved and diluted (1:20) in PBS buffer, pH 7.4, and then used for fluorescence spectroscopy. The contents of DT, prKYN, and prN-FKYN were estimated on the basis of their characteristic fluorescence at the wavelengths of 330/415, 365/480, and 325/434 nm, respectively (Diplock et al. 1991).

Assays of lipid peroxidation markers

Lipid hydroperoxides Lipid hydroperoxide (L-OOH) levels were determined spectrophotometrically by the method that uses oxidation of ferrous ions with xylenol orange (ferrous oxidation with xylenol orange, version 2 (FOX2)) (Wolff 1994). L-OOHs oxidized ferrous to ferric ions selectively in dilute acid, and the resultant ferric ions were determined by using ferric-sensitive dye which represents the concentration of L-OOHs (Wolff 1994). Xylenol orange binds to ferric ions with high selectivity to produce a colored (blue-purple) complex. Fifty-microliter aliquots of supernatant were transferred into microcentrifuge reaction vials. FOX2 reagent (950 μL) was then added, and the samples were mixed on vortex. After incubation with FOX2 reagent at room temperature for 30 min, the samples were centrifuged at 3000*g* at 20 °C for 10 min, the resulting supernatant was carefully transferred into microplate wells, and absorbance was recorded at 560 nm against reagent blank. The coefficients of intra- and inter-assay variations were 2.1 % (n=8) and 2.3 % (n=10), respectively.

Malondialdehyde One of the major secondary products of lipid peroxidation is malondialdehyde (MDA). MDA along with other byproducts reacts with thiobarbituric acid to generate a colored product, which absorbs maximally at 535 nm, representing the color produced by all

the thiobarbituric acid reactive substances (TBARS). The rate of lipid peroxidation was determined by the procedure of Buege and Aust (1978), with slight modifications comprising only volumetric changes proportionally. The pretreatment of samples to avoid the possible interferences derived from supernatant constituents was performed according to Lykkesfeldt (2001). Ten-microliter supernatant was placed in a microcentrifuge tube; 500 μL of 42 mmol/L H_2SO_4 was then added and mixed gently, and after that, 125 μL of 100 g/L phosphotungstic acid was added and vortex-mixed. After 5 min at the room temperature, the mixture was centrifuged (3 min at 6000*g*). MDA is associated with the lipoprotein and consequently was contained in the pellet. The resulting pellet was resuspended in 750 μL of 0.75 % thiobarbituric acid (TBA) and 500 μL of 30 % trichloroacetic acid (TCA) boiled for 15 min at 95 °C and then cooled, the mixture was centrifuged at 3000*g* for 5 min, and the absorbance of supernatant was read at 532 nm against a reagent blank. Intra-assay variation of MDA assay is controlled by duplicate samples in order to obtain more precise test results. The concentration of MDA in plasma was calculated using molar extinction coefficient (ε=31,500 M^{-1} cm^{-1}) and is expressed as micromole per milligram protein. The coefficients of intra- and inter-assay variations for MDA assay were 3.4 % (n=10) and 5.2 % (n=10), respectively.

Conjugated dienes Conjugated diene (CD) levels were determined with the CD method of Francesco and Sabastiano (1994). We have made some volumetric previously established method modifications to the previous method which gave increased sensitivity and high reproducibility to the CD assay by minimizing disadvantage of the background effect. At first, tissue lipids were isolated from homogenate samples according to the method of Folch et al. (1957). The samples were mixed with chloroform/methanol (2:1 *v*/*v*) reagent to a final volume, 20 times to the volume of the sample at first. Then, the whole mixtures were placed in an orbital shaker at the room temperature for 15 min. Resulting samples were centrifuged to recover the liquid phase. The solvents were washed with 4 mL of serum physiologic solution. After a few seconds of vortexing, the mixtures were centrifuged at 2000*g* to separate two phases. Upper phases were removed, and the lower chloroform phases containing lipids were evaporated under a nitrogen stream. After the evaporation stage, the samples were dissolved in cyclohexane. All the samples were subjected to spectral scanning between 230 and 250 nm to determine wavelength peaks between 230 and 260 nm. Both CDc,t and CDt,t present distinct absorbance at 242 and 233 nm, respectively. CDs detected in tissue lipid extracts were improved by second derivative spectrophotometry by using the following formula:

$$^{n}D_{x\lambda} = d^{n}A/d\lambda^{n} = f(\lambda) \text{ or } ^{n}D_{x,v} = d^{n}A/dv^{n} = f(v)$$

expressing n as the derivative order, $^{n}D_{x\lambda}$ or $^{n}D_{x,v}$ as the value of an order derivative of an analyte (x), λ as the analytical wavelength, v as the wavelength number, and A as the absorbance (Karpinska 2012). The second derivative spectra showed fine spectral structures with at least three negative peaks. The wavelengths of their minima are different for CDc,t and CDt,t, geometric isomers, which allowed the determination of each individual isomer in a mixture without any separation.

Estimation of oxidative DNA damage

8-Hydroxy-2′-deoxyguanosine levels 8-Hydroxy-2′-deoxyguanosine (8-OHdG) concentrations of the myocardial tissue samples were determined by using an enzyme-linked immunosorbent assay detection kit (OXIS, Bioxytech, EIA, USA).

Estimation of antioxidant status

Cu–Zn superoxide dismutase activity Cu–Zn superoxide dismutase (Cu–Zn-SOD) (EC 1.15.1.1) activity was measured by using the method of Sun et al. (1988), with some volumetric modifications. This method involves the inhibition of nitroblue tetrazolium (NBT) reduction, with xanthine oxidase (XO) used as a superoxide generator. Enzyme activity was determined by measuring the inhibition rate of substrate hydrolysis in the assay mixture containing 0.3 mmol/L xanthine, 0.6 mmol/L Na_2EDTA, 150 μmol/L NBT, 400 mmol/L Na_2CO_3, and 1 g/L BSA. The pH value of the assay mixture was adjusted to pH 10.2. Nine hundred seventy-two-microliter assay mixture and 13 μL XO (167 U/L) were added into 25 μL of the sample. At the end of the 20-min incubation period, 250-μL 0.8 mmol/L $CuCl_2$ was added to the microplate wells in order to terminate reaction. The final absorbance was recorded at 560 nm against a reagent blank. The inhibition rate percent was

calculated according to the following equation: $A_{blank} - A_{sample}/A_{blank} \times 100$. One unit of Cu–Zn SOD is defined as the amount of enzyme needed to exhibit a 50 % dismutation of superoxide radical anion.

Ferric reducing/antioxidant power assay Tissue antioxidant status was evaluated using ferric reducing/antioxidant power (FRAP) assay (Benzi and Strain 1999): The modified FRAP assay uses antioxidants as reductants in a redox-linked colorimetric method. In this assay, at low pH, a ferric-2,4,6-tripyridyl-*s*-triazine (Fe^{III}-TPTZ) complex was reduced to the ferrous form, which was blue-colored and monitored by measuring the change in absorption at 593 nm. The change in absorbance is directly proportional to the reducing power of the electron-donating antioxidants present in the plasma. Three hundred micromoles per liter of acetate buffer (pH 3.6), 10 mmol/L TPTZ in 40 mmol/L HCl, and 20 mmol/L $FeCl_3 \cdot 6H_2O$ in the ratio of 10:1:1 give the working FRAP reagent. Fe(II) standards were used. Fe(II) (1000 μmol/L) is equivalent to 1000 μmol/L of FRAP. Seven hundred fifty microliters of working FRAP reagent was mixed with 25 μL sample or standard in a test tube. The absorbance at 593 nm was recorded against a reagent blank. The absorbance change was converted into a FRAP value in millimolar by relating the change of absorbance at 593 nm of the test sample to that of the standard solution of known FRAP value (3–0.375 mM). The coefficients of intra- and inter-assay variations for modified FRAP assay were 1.6 % (n=8) and 2.8 % (n=8), respectively.

Total thiol and nonprotein thiol groups The concentration of redox-sensitive thiol group containing biomarkers such as myocardial T-SH and NP-SH concentrations was analyzed by using 5,5-dithiobis(2-nitrobenzoic acid) (DTNB) as described by Sedlak and Lindsay (1968). We realized some slight modifications from the previously described T-SH method in order to apply small volumes of samples. A part (20 μL) of the supernatant was mixed in 1.5-mL test tube with 400 μL of 0.2 M Tris buffer, pH 8.2, and 20 μL of 0.01 M DTNB for the determination of T-SH groups. NP-SH samples were assayed in the following way: 20 μL of supernatant was mixed in 400 μL of 50 % trichloroacetic acid. The tubes were vortexed intermittently for 10 min and centrifuged at 3000*g* for 15 min. Supernatant fractions were assayed for T-SH. The absorbance values of the resulting samples were recorded at 412-nm wavelength against a reagent blank. The value of molar extinction coefficient of thiol groups at wavelength 412 nm is ε=13,100 M^{-1} cm^{-1}. The coefficients of intra- and inter-assay variations were 1.4 % (n=8) and 3.8 % (n=9), respectively.

Estimation of total protein content

Protein contents of the samples were determined by using fluorometric protein Qubit assay kit (Life Technologies, New York, USA).

Data processing

Statistical calculations were performed using SPSS software (ver. 20.0, SPSS, Chicago, IL, USA). Data were expressed as the mean±SEM for each group. Kruskal–Wallis nonparametric ANOVA test was used to compare samples. Post hoc tests were conducted by the Bonferroni–Dunn test. p values <0.05 were regarded as statistically significant. The second derivative calculations were performed using MATLAB software (MathWorks 2010: Natick, MA, USA).

Results

Our current results show that the MA group shares significant similarities both histologically and biochemically with the NA rats. When the results of these 16 parameters were compared statistically between the groups MA and NA, no significant difference was seen; hence, the levels of the parameters standing for the antioxidant status, SOD, T-SH, and NP-SH, and the levels of P-SH and 8-OHdG parameters being the markers for oxidative stress were seen significantly lower when considered in mean in the NA group, yet this is not statistically significant. Detailed histological comments related to myocardial tissue of naturally and MA rats with their YCs were given in Fig. 1a–i.

Histological comments related to young controls

Myocardial tissue of YCs can be viewed as a total of branching heart muscle fibers. Nucleus of the cardiac muscle cell was centrally localized. Cytoplasm shows cross striation due to special organization of

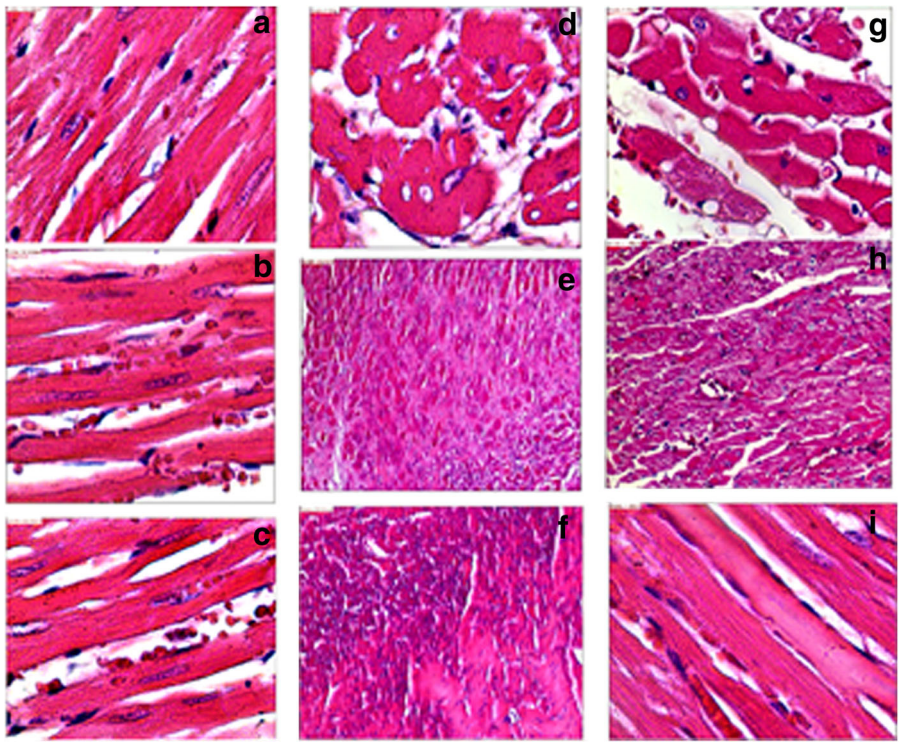

Fig. 1 Histological evaluation of the myocardial tissue of chronologically and mimetically aged rats and their young controls. Histological evaluation of the myocardial tissue of young control rats. **a**–**c** Branching muscle fibers can be observed. Centrally localized nuclei and cross striation can also be seen very clearly (H&E ×40). Connective tissue rich in capillaries can be seen between fibers (H&E ×40). Histological evaluation of the myocardial tissue of chronologically aged rats. **d** Cell cytoplasms have lots of vacuoles in cross section of the cardiac myocytes. Prominent intercellular edema is present, as well (H&E ×40). **e** Muscle fibers are replaced by spreading connective tissue (H&E ×40). **f** Degenerated muscle fibers with no visible myofilaments cover a wide area (HE ×40). Histological evaluation of the myocardial tissue of mimetically aged rats. **g** Cell cytoplasms have lots of vacuoles in cross section of the cardiac myocytes. Intercellular edema is attracting attention, as well. Cytoplasmic loss of myofibers is noticed (HE ×40). **h** Randomly and sparsely distributed myofibers are giving their places into connective tissue (HE ×10). **i** Degenerated, pale myofibers accompanied with disappearance of myofilaments are seen (H&E ×40)

myofilaments and also longitudinal striation due to the parallel array of myofibers. Intercalated disks between adjacent cells can also be observed. Fibers were surrounded by loose connective tissue rich in capillaries. Detailed histological comments related to YCs are given in Fig. 1a–c.

Histological comments related to naturally aged group

The most striking histopathological alteration occurred in this group was "vacuolization." Especially in cross sections, cell cytoplasms have many vacuoles. Intercellular edema is grabbing attention, as well. In some areas, disappearance of myofilaments and pale appearance of cytoplasms are observed. In addition to all aforementioned features, necrotic muscle cells are also noticed. Some microscopic areas have high amount of connective tissue. Detailed histological comments related to NA group are given in Fig. 1d–f.

Histological comments related to mimetically aged group

The prominent histopathological changes that we observed in this group are vacuolization, just like the chronological aging group. Cell cytoplasms have lots of vacuoles particularly prominent in cross sections. Intercellular edema is taking attention, as well. In some areas, disappearance of myofilaments and pale appearance of cytoplasms are observed. In addition to all previous features, necrotic muscle cells were also noticed. Some microscopic areas have high amount of connective tissue. Detailed histological comments related to MA group are given in Fig. 1g–i.

Results related to oxidative stress parameters

General and specific protein oxidation biomarkers

The myocardial general and specific protein oxidation biomarker profiles of NA, MA, and YC rats are given in Figs. 2a–c and 3a–d, respectively. As a general protein oxidation biomarker profile, AOPP, PCO, prAGE, and also specific protein oxidation biomarkers as P-SH, prDT, prKYN, and prN-FKYN concentrations in MA and NA rats were found to be significantly higher compared to those in YC rats. On the other hand, the levels of P-SH were not significantly different between groups.

Lipid peroxidation biomarkers

Figure 4a–d shows the effect of mimetic aging on myocardial lipid peroxidation biomarkers, such as L-OOH, MDA, and CD in MA and NA rats that were found to be significantly higher in comparison to those in YCs.

Oxidative DNA damage biomarker

8-OHdG concentrations of the myocardial tissue of NA rats, MA rats, and their corresponding YCs are given in Fig. 5. The 8-OHdG concentrations of myocardial tissue were significantly different between NA rats and the YC group. There was also a significant difference between MA rats and the YC group.

Antioxidant capacity biomarkers

Antioxidant capacity biomarkers in myocardial tissue of both experimental groups and their corresponding YCs are given in Fig. 6a–d. As an antioxidant status in the MA and NA groups, Cu–Zn SOD, FRAP, and T-SH levels were lower than those in the YCs. Only NP-SH levels were not significantly different among groups.

Discussion

The cardiac senescence and age-related disease progression have gained general attention and recognition in the past decades due to the increased accessibility and quality of health care. The advancement in global civilization is complementary regarding elderly population and development of chronic age-related disorders (Siddiqi and Sussman 2013). Post-mitotic cells such as brain and heart tissues are particularly vulnerable to deteriorated age-related redox homeostasis (Çakatay 2010). The current aging model was first reported in China that injection of a low dose of D-galactose into mice could induce changes which resembled accelerated aging. The aging model shows neurological impairment, decreased activity of antioxidant enzymes, and poor immune responses (Song et al. 1999). However, the underlining mechanism remains largely unknown. To our knowledge, this is the first article related to the effects of D-galactose-induced accelerated aging on histopathological changes and redox homeostasis of the cardiac muscle in the current literature.

The main histomorphological changes during aging happen in the structure of cardiac tissue, in the conduction system, and in vessels. Hydroxyl radicals have damaging effect on the protein structure in cardiac mitochondria, myofibrils (Babusıkova et al. 2004; Judge et al. 2005), and sarcoplasmic reticulum (Kaplan et al. 2003) in adult rats. Babusıkova et al. (2008) have shown that oxidative damage in proteins and lipids of cardiac sarcoplasmic reticulum increases during in vitro-generated oxidative stress in senescent rats. It has been suggested that the accumulation of oxidant-induced damage in interfibrillar mitochondria may be a major contributing factor to the age-related alterations in myocardial function (Judge et al. 2005). ROS in cells are formed as a result of defects in coupled electron transport within mitochondria. The overproduction of ROS could cause a wide spectrum of oxidative damage to various subcellular components including plasma membrane, organelles, and DNA, which would lead to cell death, or elicit apoptosis by inducing changes in mitochondrial membrane permeability (Meissner 2007). Vacuole formation and cell swelling are the earliest reversible reactions of cells against damaging factors that result in alterations of the cell membrane permeability (Eşrefoglu et al. 2011). The aforementioned ultrastructural changes also include interstitial edema and the appearance of intracellular vacuoles in cardiac myocytes of chronologically aged rats. They also observed prominent myofilament disruption and disorganization as well as mitochondrial degeneration in aged rats. In our study, we clearly observed similar histopathological and oxidative stress-related changes in the myocardial tissue of NA and MA rats. Our current experimental findings indicate that histopathological degeneration and impaired redox homeostasis in myocardial tissue could be a primarily

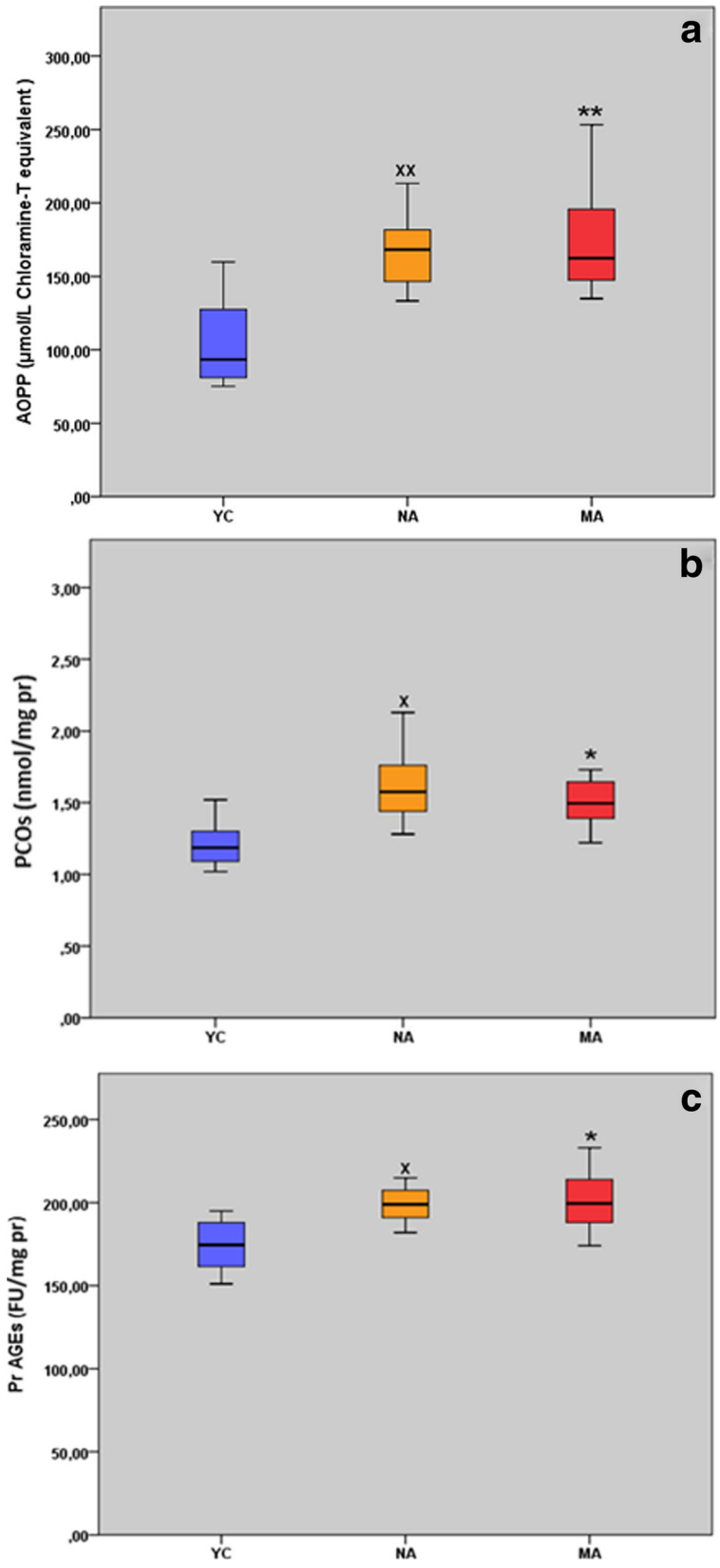

Fig. 2 General protein oxidation biomarkers in myocardial tissue of naturally aged rats (*NA*; $n=8$), mimetically aged rats (*MA*; $n=8$), and their corresponding young controls (*YC*; $n=8$). Results were expressed as mean±SEM. Data were statistically different between groups (*$p<0.05$; **$p<0.01$; YC vs MA) ($^{x}p<0.05$; $^{xx}p<0.01$; YC vs NA). *PCO* protein carbonyl groups, *AOPP* advanced oxidation protein end products, *prAGEs* protein-bound advanced glycation end products

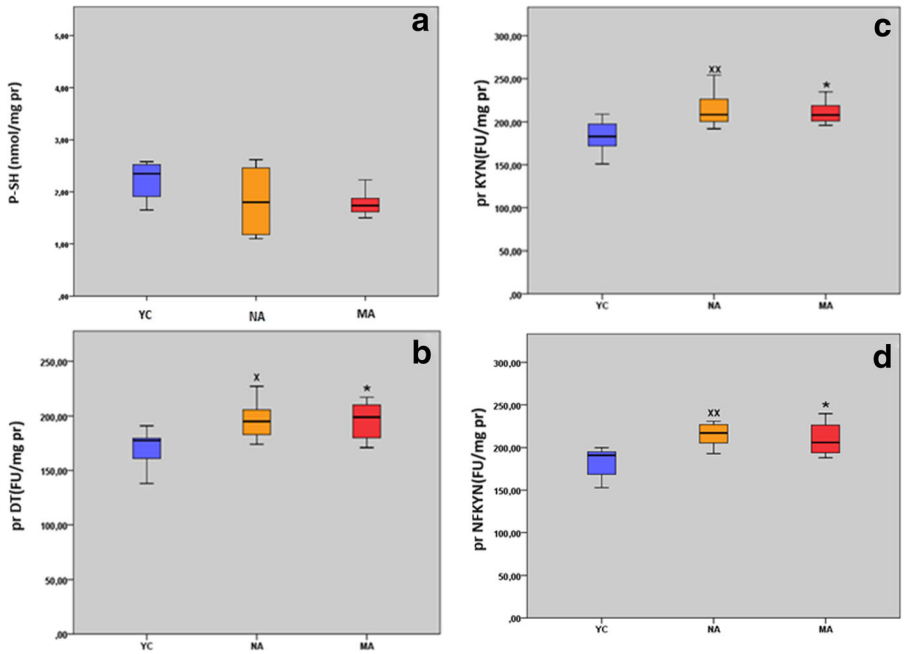

Fig. 3 Specific protein oxidation biomarkers in the myocardial tissue of naturally aged rats (*NA*; $n=8$), mimetically aged rats (*MA*; $n=8$), and their corresponding young controls (*YC*; $n=8$). Results were expressed as mean±SEM. Data were statistically different between groups (*$p<0.05$; YC vs MA) ($^{x}p<0.05$; $^{xx}p<0.01$; YC vs NA). *P-SH* protein thiol, *prDT* protein-bound dityrosine, *prKYN* protein-bound kynurenine, *prN-FKYN* protein-bound *N*′-formylkynurenine

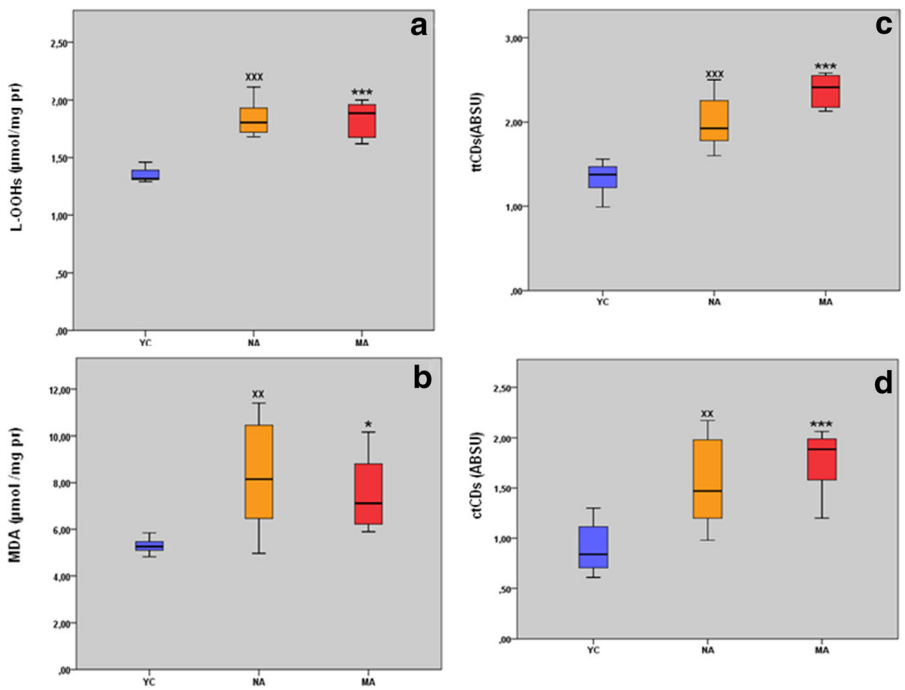

Fig. 4 Lipid peroxidation biomarkers in myocardial tissue of naturally aged rats (*NA*; $n=8$), mimetically aged rats (*MA*; $n=8$), and their corresponding young controls (*YC*; $n=8$). Results were expressed as mean±SEM. Data were statistically different between groups (*$p<0.05$; ***$p<0.001$; YC vs MA) ($^{xx}p<0.01$; $^{xxx}p<0.001$; YC vs NA). *MDA* malondialdehyde, *L-OOHs* lipid hydroperoxides, *ttCDs* trans-trans conjugated diens, *ctCDs* cis–trans-conjugated diens

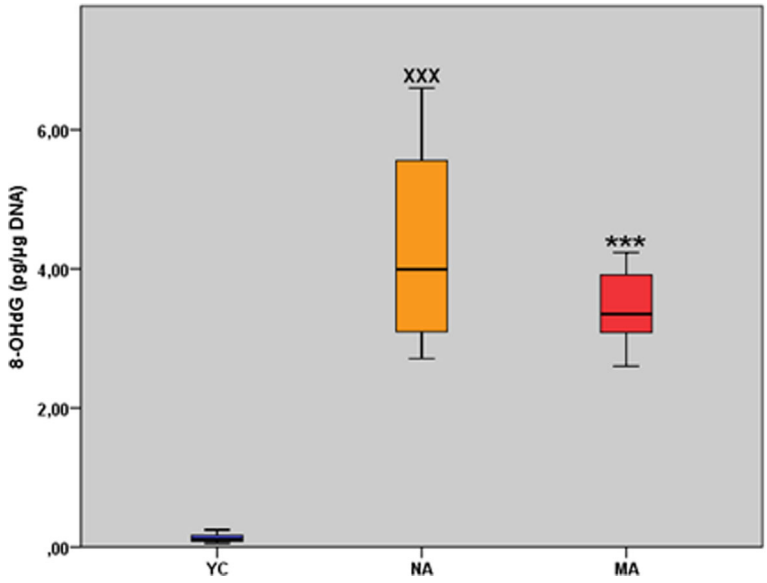

Fig. 5 8-Hydroxy-2′-deoxyguanosine concentrations of the myocardial tissue of naturally aged rats (*NA*; n=8), mimetically aged rats (*MA*; n=8), and their corresponding young controls (*YC*; n=8). Results were expressed as mean±SEM. Data were statistically different between groups (***p<0.001; YC vs MA) (^{xxx}p<0.001; YC vs NA). *8-OHdG* 8-hydroxy-2′-deoxyguanosine

etiological sign of D-galactose-induced accelerated cardiac senescence.

Our results related to MA group share significant similarities in terms of impaired redox homeostasis when compared to NA rats. Cellular thiol fractions such as T-SH, P-SH, and NP-SH are the major antioxidant systems in cardiac tissue and consequently play a critical role in protecting against oxidative damage. Here, we show for the first time that myocardial P-SH levels remain unchanged with both experimental aging groups due to its critical redox buffer role to maintain protein redox homeostasis. A strong relationship among L-

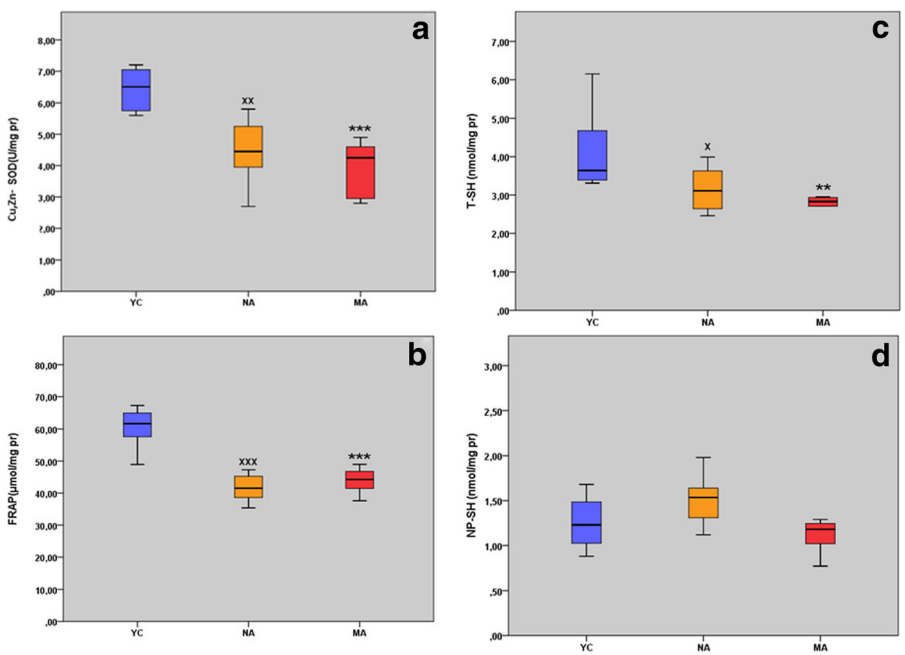

Fig. 6 Antioxidant capacity biomarkers in myocardial tissue of naturally aged rats (*NA*; n=8), mimetically aged rats (*MA*; n=8), and their corresponding young controls (*YC*; n=8). Results are expressed as mean±SEM. Data were statistically different between groups (**p<0.01; ***p<0.001; YC vs MA) (^{x}p<0.05; ^{xx}p<0.01; ^{xxx}p<0.001; YC vs NA). *Cu–Zn SOD* Cu–Zn superoxide dismutase, *FRAP* ferric reducing antioxidant power, *T-SH* total thiol groups, *NP-SH* nonprotein thiol groups

OOH, MDA, and CD has been reported in the current literature (Cebe et al. 2014). CDs and L-OOHs are the initial products of lipid peroxidation, and they are formed by omega-6 polyunsaturated fatty acids that react with ROS (Eaton et al. 2001; Wolff 1994). The reactivity of L-OOHs could be defined as the damaging ability of tissue proteins. It was also shown that these reactive species applied exogenously participate in the occurrence of cardiac dysfunction (Eaton et al. 2001). L-OOH is produced in myocardial tissue during impaired oxidative state, and it has the ability to elicit cardiac dysfunction. It is also possible that L-OOH-modifying cardiac proteins cause cardiac dysfunction and probably accompany with myocardial aging process. The reactive lipid aldehydes such as MDA and their derivatives are detoxified via a variety of phase 1 and phase 2 systems. When antioxidant defenses are compromised or oxidative conditions are increased, protein carbonylation process (a formation of the PCO groups) is probably increased (Baraibar et al. 2012). Identifying the carbonylated proteins is crucially important for assessing cellular redox homeostasis, and they could potentially provide important information about molecular mechanisms underlying the progression of aging process and occurrence of age-related disorders linked to increased oxidative stress. In our research, significant increase was observed in MA group concerning MDA, which is the final reactive product of lipid peroxidation. We think that the aforementioned situation may lead to possible outcomes in MA group: Since MDAs are the secondary reactive products of lipid peroxidation, with the increasing oxidative damage, these formed reactive aldehydes transform into reactive aldehyde-protein adducts giving out PCOs by secondary modification reactions (Eşrefoglu et al. 2011), which elevated tissue MDA levels in the heart and thoracic aorta of chronologically aged rats.

AOPPs are formed during chronic oxidative stress as a result of reactions between proteins and reactive oxidants. Their levels are elevated during various cardiovascular diseases (Valente et al. 2013). Elevated AOPPs serve as independent risk factors for ischemic heart disease and cardiomyocyte death, which is a hallmark of ischemic heart disease (Valente et al. 2013). AOPP contains a variety of oxidation products such as PCOs, prDT, and AGE-pentosidine. DT is a fluorescent molecule and one of the cross-linkers of cellular proteins which is formed by the reaction of two tyrosyl radicals following the oxidation of tyrosine (DiMarco and Giulivi 2007). We conclude that the increase in PCO/AOPP, DT/AOPP, and prAGEs/AOPP ratio may contribute a partial increase in AOPP levels in NA and MA groups. On the other hand, we are of the conviction that the increased lipid peroxidation rate which appears to occur in both experimental groups of rats may be an enhancing factor in the propagation of protein oxidation, as indicated by the increased PCO and AOPP levels in cardiac tissue.

It has been previously shown that Cu–Zn SOD activities in the serum and kidney tissues of experimental animals are regulated by the aging process (Cebe et al. 2014; Comai et al. 2005). Persistent oxidative stress related to lower FRAP and decreased activity of Cu–Zn SOD observed in MA and NA rats may contribute enhanced susceptibility for oxidative damage in the myocardial tissue.

No established data or mechanistic explanation exists in current literature that focuses on how D-galactose administration induces oxidative DNA damage with the increase of 8-OHdG formation in myocardial tissue of MA group. The mitochondrial dysfunction caused by complex I deficiency in MA rats may lead to increased free radical formation and oxidative modification of DNA bases. It is well known that oxidative damage of DNA can accelerate telomere shortening and contribute to aging process (Tzanetakou et al. 2013). Whatever the mechanism is, the observation that 8-OHdG increases as a part of the D-galactose-induced aging response is important. It has been also reported that chronic administration of D-galactose may increase DNA mutations in the mitochondria (Zhong et al. 2011). On the other hand, oxidative damage of histone proteins could induce DNA damage in MA rats.

Conclusion and future directions

Whether the source of ROS is endogenous or exogenous impaired the redox homeostasis detrimental for all post-mitotic organs such as the heart. Discovery of relevant biomarkers in order to differentiate chronological aging from biological and/or accelerated aging contributes to the current literature of experiment-based evidence on the oxidative stress theory of aging. Our current results show that experimentally induced accelerated aging model could be considered as a reliable experimental model for mimetic aging of cardiac tissue. The current research could also enlighten other biogerontologists on

the perspective of accelerated aging models, oxidant power on senescence in vivo-generated glyoxidative stress, and possible regulative role of endogenous antioxidant systems on aging. We also think that other experimental aging models like jet lag and antiaging models like calorie restriction can be compared with our results in the near future for a better understanding for the concepts of the aging molecular mechanisms.

The current study is novel and a nominee to be the first experimental study in the literature implying the effect of D-galactose on histopathological changes in the myocardial tissue which is similarly seen in natural aging. Our aim is to plan new studies enlightening apoptosis, autophagy, and mitochondrial ultrastructure with immunohistochemical methods related to mimetic aging in the future. Additional studies are warranted to clarify the potential involvement of these oxidative changes as mechanistic factors in the association of accelerating aging with age-related myocardial disorders.

Acknowledgments This study was supported partially by TUBITAK (2209) research grant and Istanbul University research grant (UDP-34391).

Authorship and disclosures UÇ, SA, and PA were the principal investigators and mentors who took primary responsibility for the research. KY, TC, AIK, TO, AK, MM, and MES also took responsibility for housing, care, and maintenance of experimental animals and made contributions to work at the laboratory. Histological evaluations were made by MŞA, ME, and KY who performed the statistical analysis and prepared the figures. UÇ, KY, and PA wrote the paper principally, and AK made contributions to the first draft. All the authors read and approved the final manuscript.

Conflict of interest The authors reported no conflicts of interest.

References

Aydın S, Yanar K, Atukeren P, Dalo E, Sitar ME, Uslu E, Caf N, Çakatay U (2012) Comparison of oxidative stress biomarkers in renal tissues of D-galactose induced, naturally aged and young rats. Biogerontology 13:251–260. doi:10.1007/s10522-011-9370-3

Babusıkova E, Kaplan P, Lehotsky J, Jesenak M, Dobrota D (2004) Oxidative modification of rat cardiac mitochondrial membranes and myofibrils by hydroxyl radicals. Gen Physiol Biophys 23:327–335

Babusıkova E, Jesenak M, Dobrota D, Tribulova N, Kaplan P (2008) Age-dependent effect of oxidative stress on cardiac sarcoplasmic reticulum vesicles. Physiol Res 57:S49–S54

Baraibar MA, Liu L, Ahmed EK, Friguet B (2012) Protein oxidative damage at the crossroads of cellular senescence, aging, and age-related diseases. Oxidative Med Cell Longev 2012: 919832. doi:10.1155/2012/919832

Benzi IF, Strain JJ (1999) Ferric reducing/antioxidant power assay: direct measure of total antioxidant activity of biological fluids and modified version for simultaneous measurement of total antioxidant power and ascorbic acid concentration. Methods Enzymol 299:15–27. doi:10.1016/S0076-6879(99)99005-5

Buege JA, Aust SD (1978) Microsomal lipid peroxidation. Methods Enzymol 52:302–310

Çakatay U (2010) Protein redox-regulation mechanisms in aging. In: Bondy SC, Maise K (eds) Aging and age-related disorders. Humana Press Inc., New York, pp 1–24. doi:10.1007/978-1-60761-602-3_1

Cebe T, Atukeren P, Yanar K, Kuruç AI, Ozan T, Kunbaz A, Sitar ME, Mirmaroufizibandeh R, Aydın S, Cakatay U (2014) Oxidation scrutiny in persuaded aging and chronological aging at systemic redox homeostasis level. Exp Gerontol 57C:132–140. doi:10.1016/j.exger.2014.05.017

Choksi KB, Papaconstantinou J (2008) Age-related alterations in oxidatively damaged proteins of mouse heart mitochondrial electron transport chain complexes. Free Radic Biol Med 44: 1795–1805. doi:10.1016/j.freeradbiomed.2008.01.032

Comai S, Bertazzo A, Ragazzi E, Caparrotta L, Costa CV, Allegri G (2005) Influence of age on Cu/Zn-superoxide dismutase and indole 2,3-dioxygenase activities in rat tissues. Ital J Biochem 54:232–239

DiMarco T, Giulivi C (2007) Current analytical methods for the detection of dityrosine, a biomarker of oxidative stress, in biological samples. Mass Spectrom Rev 26:108–120. doi:10.1002/mas.20109, Review

Diplock AT, Symons MCR, Rice-Evans C (1991) Techniques in free radical research. Elsevier Science, Tokyo

Duicu OM, Mirica SN, Gheorgheosu DE, Privistirescu AI, Fira-Mladinescu O, Muntean DM (2013) Ageing-induced decrease in cardiac mitochondrial function in healthy rats. Can J Physiol Pharmacol 91:593–600. doi:10.1139/cjpp-2012-0422

Eaton P, Hearse DJ, Shattock MJ (2001) Lipid hydroperoxide modification of proteins during myocardial ischaemia. Cardiovasc Res 51:294–303. doi:10.1016/S0008-6363(01)00303-0

Eşrefoglu M, Gul M, Ateş M, Erdoğan A (2011) The effects of caffeic acid phenethyl ester and melatonin on age-related vascular remodeling and cardiac damage. Fundam Clin Pharm 25:580–590. doi:10.1111/j.1472-8206.2010.00876.x

Fanin J, Rice KM, Thulluri S, Arvapalli RK, Wehner P, Blough ER (2013) The effects of aging on indices of oxidative stress and apoptosis in the female Fischer 344/Nnia X Brown Norway/BiNia rat heart. Open Cardiovasc Med J 29:113–121. doi:10.2174/1874192401307010113

Folch J, Lees M, Sloane Stanley GH (1957) A simple method for the isolation and purification of total lipides from animal tissues. J Biol Chem 226:497–509

Francesco P, Sabastiano B (1994) Detection of conjugated dienes by second derivative ultraviolet spectrophotometry. Methods

Enzymol 233:303–310. doi:10.1016/S0076-6879(94)33033-6

Hanasand M, Omdal R, Norheim KB, Gøransson LG, Brede C, Jonsson G (2012) Improved detection of advanced oxidation protein products in plasma. Clin Chim Acta 413:901–906. doi:10.1016/j.cca.2012.01.038

Jin K (2010) Modern biological theories of aging. Aging Dis 1:72–74

Judge S, Jang YM, Smith A, Hagen T, Leeuwenburgh C (2005) Age-associated increases in oxidative stress and antioxidant enzyme activities in cardiac interfibrillar mitochondria: implications for the mitochondrial theory of aging. FASEB J 19:419–421. doi:10.1096/fj.04-2622fje

Kaplan P, Babusikova E, Lehotsky J, Dobrota D (2003) Free radical-induced protein modification and inhibition of Ca2+-ATPase of cardiac sarcoplasmic reticulum. Mol Cell Biochem 248:41–47

Karpinska J (2012) Basic principles and analytical application of derivative spectrophotometry. In: Jamal U (ed) Macro to nano spectroscopy. Intech, Rijeka, p 13

Kumar D, Rizvi SI (2014) Plasma paraoxonase 1 arylesterase activity in D-galactose-induced aged rat model: correlation with LDL oxidation and redox status. Aging Clin Exp Res 26:261–267. doi:10.1007/s40520-013-0170-2

Lenarczyk M, Cohen EP, Fish BL, Irving AA, Sharma M, Driscoll CD, Moulder JE (2009) Chronic oxidative stress as a mechanism for radiation nephropathy. Radiat Res 171:164–172. doi:10.1667/RR1454.1

Lykkesfeldt J (2001) Determination of malondialdehyde as dithiobarbituric acid adduct in biological samples by HPLC with fluorescence detection: comparison with ultraviolet-visible spectrophotometry. Clin Chem 47:1725–1727

Meissner C (2007) Mutations of mitochondrial DNA—cause or consequence of the ageing process? Z Gerontol Geriatr 40:325–333. doi:10.1007/s00391-007-0481-z

Munch G, Kies R, Wessel A, Riederer P, Bahner U, Heidland A, Niwa T, Lemke HD, Schinzel R (1997) Determination of advanced glycation end products in serum by fluorescence spectroscopy and competitive ELISA. Eur J Clin Chem Clin Biochem 35:669–677

Reznick AZ, Packer L (1994) Oxidative damage to proteins: spectrophotometric method for carbonyl assay. Method Enzymol 233:357–363. doi:10.1016/S0076-6879(94)33041-7

Sedlak J, Lindsay RH (1968) Estimation of total, protein-bound, and nonprotein sulfhydryl groups in tissue with Ellman's reagent. Anal Biochem 25:192–205

Shinmura K (2013) Effects of caloric restriction on cardiac oxidative stress and mitochondrial bioenergetics: potential role of cardiac sirtuins. Oxidative Med Cell Longev. doi:10.1155/2013/528935 [Epub ahead of print]

Siddiqi S, Sussman MA (2013) Cardiac hegemony of senescence. Curr Transl Geriatr Exp Gerontol Rep 2:247–254. doi:10.1007/s13670-013-0064-3

Sitar ME, Yanar K, Aydın S, Çakatay U (2013) Current aspects of ageing theories and classification according to mechanisms. Turk J Geriatr 16:339–346

Song X, Bao M, Li D, Li YM (1999) Advanced glycation in D-galactose induced mouse aging model. Mech Ageing Dev 108:239–251

Sudheesh NP, Ajith TA, Ramnath V, Janardhanan KK (2010) Therapeutic potential of *Ganoderma lucidum* (Fr.) P. Karst. against the declined antioxidant status in the mitochondria of post-mitotic tissues of aged mice. Clin Nutr 29:406–412. doi:10.1016/j.clnu.2009.12.003

Sun Y, Oberley LW, Li Y (1988) A simple method for clinical assay of superoxide dismutase. Clin Chem 34:497–500

Sung MM, Dyck JR (2012) Age-related cardiovascular disease and the beneficial effects of calorie restriction. Heart Fail Rev 17:707–719. doi:10.1007/s10741-011-9293-8

Tzanetakou IP, Nzietchueng R, Perrea DN, Benetos A (2014) Telomeres and their role in aging and longevity. Curr Vasc Pharmacol 12(5):726–734

Uzun D, Korkmaz GG, Sitar ME, Cebe T, Yanar K, Cakatay U, Aydın S (2013) Oxidative damage parameters in renal tissues of aged and young rats based on gender. Clin Interv Aging 8:809–815. doi:10.2147/CIA.S46188

Valente AJ, Yoshida T, Clark RA, Delafontaine P, Siebenlist U, Chandrasekar B (2013) Advanced oxidation protein products induce cardiomyocyte death via Nox2/Rac1/superoxide-dependent TRAF3IP2/JNK signaling. Free Radic Biol Med 60:125–135. doi:10.1016/j.freeradbiomed.2013.02.012

Venkataraman K, Khurana S, Tai T (2013) Oxidative stress in aging—matters of the heart and mind. Int J Mol Sci 14:17897–17925. doi:10.3390/ijms140917897

Wolff SP (1994) Ferrous ion oxidation in presence of ferric ion indicator xylenol orange for measurement of hydroperoxides. Methods Enzymol 233:182–189. doi:10.1016/S0003-2697(02)00606-1

Wróbel K, Wróbel K, Garay-Sevilla ME, Nava LE, Malacara JM (1997) Novel analytical approach to monitoring advanced glycosylation end products in human serum with on-line spectrophotometric and spectrofluorometric detection in a flow system. Clin Chem 43:1563–1569

Yanar K, Aydın S, Çakatay U, Mengi M, Buyukpınarbaş N, Atukeren P, Sitar ME, Sönmez A, Uslu E (2011) Protein and DNA oxidation in different anatomic regions of rat brain in a mimetic ageing model. Basic Clin Pharmacol Toxicol 109:423–433. doi:10.1111/j.1742-7843.2011.00756.x

Zeng JH, Zhong ZM, Li XD, Wu Q, Zheng S, Zhou J, Ye WB, Xie F, Wu XH, Huang ZP, Chen JT (2014) Advanced oxidation protein products accelerate bone deterioration in aged rats. Exp Gerontol 50:64–71. doi:10.1016/j.exger.2013.11.014

Zhong Y, Hu YJ, Yang Y, Peng W, Sun Y, Chen B, Huang X, Kong WJ (2011) Contribution of common deletion to total deletion burden in mitochondrial DNA from inner ear of D-galactose-induced aging rats. Mutat Res 712:11–19. doi:10.1016/j.mrfmmm.2011.03.013